Angle-resolved photoemission study of dispersive and narrow-band 5*f* states in UAsSe

E. Guziewicz,[1,2,*] T. Durakiewicz,[1] P. M. Oppeneer,[3] J. J. Joyce,[1] J. D. Thompson,[1] C. G. Olson,[4] M. T. Butterfield,[5] A. Wojakowski,[6] D. P. Moore,[1] and A. J. Arko[1]

[1]*Los Alamos National Laboratory, Los Alamos, New Mexico 87545, USA*

[2]*Institute of Physics, Polish Academy of Sciences, Warsaw, Poland*

[3]*Dept. of Physics, Uppsala University, Box 530, S-751 21 Uppsala, Sweden*

[4]*Ames Laboratory, Iowa State University, Ames, Iowa 50011, USA*

[5]*Lawrence Livermore National Laboratory, Livermore, California 94550, USA*

[6]*Institute of Low Temperature and Structure Research, Polish Academy of Sciences, Wrocław, Poland*

(Received 4 July 2005; revised manuscript received 19 December 2005; published 25 April 2006)

Single crystals of ferromagnetic UAsSe have been investigated by angle-resolved photoemission spectroscopy (ARPES) in the photon energy range between 20 eV and 110 eV. Electron kinetic energy intensities are collected as a function of angle and mapped onto the materials reciprocal space. Energy-band mapping has been carried out both for a several-eV-wide energy interval as well as for a narrow energy interval of less than 1 eV from the Fermi energy. The main features of the deduced energy bands can be explained by band-structure calculations. In the interval close to the Fermi energy, the very high energy and momentum resolution allows the observation of a narrow, yet dispersive photoemission peak mainly of 5*f* character situated within 50 meV of the Fermi energy. The Lorentzian linewidth was found to be about 35 meV with a dispersion of 30 meV along the Γ to Z direction and 40 meV dispersion along the Γ to X direction in the Brillouin zone. We have also found broader (linewidth about 70 meV), hybridized *f*-character bands with a conventional dispersion of about 1 eV along the Γ to X and the Z to R directions in the Brillouin zone. An intriguing electronic structure emerges for UAsSe in which both relatively dispersive and narrow 5*f* bands are present. The occurrence of 5*f*-band dispersions stipulates that the electronic structure of UAsSe requires lattice periodicity to be taken into account.

DOI: 10.1103/PhysRevB.73.155119 PACS number(s): 79.60.−i, 71.28.+d, 74.25.Jb

I. INTRODUCTION

The *f* electrons in actinide materials are well known to exhibit an unusual dual nature: the behavior of the 5*f*'s can range—from one actinide material to another—from being localized to itinerant.[1,2] The localization or hybridization of the 5*f* electrons dominates to a large extent the physical properties, such as, e.g., large anisotropic thermal-expansion coefficients, enhanced mass, or spin and charge density waves. The peculiar character of the 5*f* electronic states largely determines also the magnetic features of actinide-based compounds. For the early actinides (Ac, Th, Pa, and U) the filling of the 5*f* shell is important for the magnetic properties; however, the filling does not determine the magnetic properties in the same way as in the early lanthanide series. A relevant parameter is the actinide-actinide spacing[1] together with the density of electronic states at the Fermi level (E_F). For larger actinide-actinide distances, the interatomic 5*f*-5*f* overlap is rather small and the 5*f* electrons create narrow bands near E_F involving features typical of band magnetism. For large separations and weak hybridizations, even atomiclike 5*f* levels may appear, leading to features characteristic of local-moment magnetism. The main attribute of the band magnetism of 5*f* compounds is the strong spin-orbit interaction, leading to large orbital moments, and exchange interactions mediated via hybridization of the 5*f* states with conduction electron states. Ferromagnetism in uranium compounds is observed typically when the U-U spacing is over 3.7 Å. The value of interionic spacing, which separates "magnetic" and "nonmagnetic" uranium compounds, is frequently called the Hill limit.[1] For smaller U-U distances the 5*f* wave functions of nearest neighbors overlap, leading to the formation of a broad 5*f* band and weakly paramagnetic behavior. For compounds with a very large U-U spacing, the direct overlap of the 5*f* states is not significant and we usually observe antiferromagnetic behavior.[1–5]

The complicated magnetic behavior of actinide compounds has been the focus of many experimental and theoretical investigations during the last few years.[6–10] Angular-resolved photoemission spectroscopy (ARPES) is a method providing extensive insight into the electronic structure of actinide compounds, particularly information about the localization of the 5*f* electronic states and their hybridization with ligand conduction bands. We used this method to study the electronic properties of UAsSe, which is an intriguing ferromagnetic material, possessing properties characteristic of localized as well as itinerant 5*f* electrons.

Uranium arsenoselenide is a metallic compound, which crystallizes in the tetragonal PbFCl-type of crystal structure, also known as the Cu_2Sb or ZrSiS structure ($P4/nmm$ space group). This type of crystallographic cell can be regarded as a stack of layers along the *c* direction, which is also the easy magnetic axis. The atoms along the *c* direction follow the sequence As-U-Se-Se-U-As, and uranium ions occupy only one crystallographic position [Ref. 11, Fig. 1(a)]. The uranium-uranium distance is reported to be between 3.977 and 4.000 Å,[12] which is above the Hill limit[1] for uranium compounds.

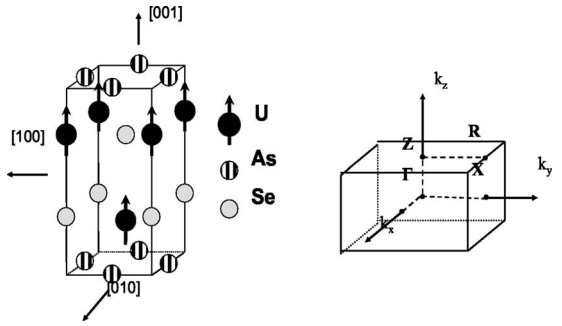

FIG. 1. (a) Crystallographic unit cell of UAsSe in the PbFCl type of crystal structure. For crystals with $T_C=108$ K, $a=3.997\pm0.001$ Å, $c=8.402\pm0.001$ Å (Ref. 12). The magnetic moments on the uranium sites are indicated by arrows. (b) Brillouin zone of UAsSe.

The layered structure of UAsSe together with the large c to a,b ratio would lead one to the consider UAsSe as a two-dimensional (2D) material. Two-dimensional systems are very attractive subjects of ARPES investigations, as E vs k dependence can be extracted from energy distribution curves (EDC's) with relative ease.

The Curie temperature T_C of UAsSe has been reported to be between 101.5 K and 118 K.[11–13] It was found that the Curie temperature strongly depends on the As/Se molar ratio and/or varies with the disorder in the anionic sublattice.[13–15] Uranium arsenoselenide is a hard ferromagnet with coercive force 0.8 T for the $\mathbf{H}\|c$ axis.[16] The magnetocrystalline anisotropy of UAsSe is very high, and the ordered moment equals $1.5\mu_B$/U.[17] The degree of $5f$ localization has been controversially discussed in the literature. Magnetic susceptibility measurements,[14,18,19] a polarized neutron diffraction study,[20] and preliminary photoemission experiments[11] appeared to favor localized $5f$ electrons in UAsSe. On the other hand, the enhanced Sommerfeld coefficient [γ is reported to be between 27.4 and 40.6 mJ/(mol K^2) (Ref. 12)] and experimental and computed magneto-optical Kerr spectra[21,22] provided evidence for a definite degree of itinerancy, at least as far as the f electrons in the U-U planes are concerned. This discrepancy of the physical results makes UAsSe an interesting actinide material, possibly combining aspects of the dual nature of $5f$ electrons in one material, and consequently, well suited for an ARPES investigation of the $5f$ states.

The electrical resistivity ρ(T) is strongly sample dependent and shows an anomalous low-temperature upturn in the magnetically ordered state, far below T_C.[12,23] The origin of this upturn has been extensively studied,[14–16,24] but not fully clarified. It has been speculated recently[13,25] that the anomaly might be related to a nonmagnetic Kondo effect generated by a small disorder in the occupation of the anion sublattice (i.e., As on Se sites and vice versa). This may be referred to a theoretical approach,[26] which relates the electrical upturn at $T=T_C/2$ to a dynamic disorder. The very small magnetoresistivity far below the ferromagnetic transition in fields up to 13.5 T points to a nonmagnetic mechanism as responsible for the unusual low-temperature transport properties observed for UAsSe.[16] Such a mechanism has been recently proposed for the isostructural compound ThAsSe.[27]

The specific heat measurements taken for off- and near-stoichiometric UAsSe crystals[16] show clear differences between electronic and lattice contributions to the low-temperature specific heat. These differences might be ascribed to the different hybridization strengths between the uranium $5f$ and the conduction electrons accompanied by a shift of the U $5f$ relative to the Fermi edge. The understanding of the role of the U $5f$ electrons in bonding and hybridization seems to be crucial for an understanding of the unusual properties of uranium arsenoselenide in particular and uranium compounds in general.

There exist only limited published photoemission data of UAsSe. The first data were taken with 200 meV energy resolution for the helium resonance lines and 1.5 eV resolution for the monochromatized $K\alpha$ magnesium characteristic line.[11] A peak found at E_F was interpreted in support of the metallic behavior of UAsSe. Enhancement of the spectral weight of this peak with increasing photon energy supported the interpretation of $5f$ character. Some preliminary angle-resolved studies of UAsSe with $T_C=113$ K were performed recently with an instrument resolution of 25 meV.[28,29] Angle-resolved data taken near the Γ point at 20 K and 40 eV photon energies showed an intense peak near the Fermi level.[28] Based on the photon energy dependence it was found that this dispersive peak is primarily of $5f$ character. It was also established[29] that the $5f$ band occupies only small parts of the Brillouin zone.

In this paper we present a comprehensive photoemission study of uranium arsenoselenide. We have focused our investigations on the uranium $5f$ level in order to specify the relationship between the U $5f$-conduction-band hybridization and shed more light on the intriguing band magnetism of actinide compounds.

A characterization of the $5f$ electrons of actinides in accordance with all the available experiments including photoemission has been a big challenge for the theory community for a number of years. A representative example is δ-Pu, which is very difficult to describe within a unified model that consistently accounts for a large volume and the absence of magnetic order[30] and is in agreement with PES results.[31–34] A possible solution seems to be given by the mixed level model[35–38] (MLM) according to which four of five $5f$ electrons are localized and form a localized multiplet while one $5f$ electron hybridizes with conduction states and forms a completely delocalized Bloch state. Although the MLM is in qualitative and quantitative agreement with experimental results for δ-Pu and some plutonium compounds [like $PuCoGa_5$ (Ref. 36)], the behavior of the $5f$ electrons still requires clarifying and new experimental results are of great interest. This is especially true for angle-resolved photoemission studies of single-crystal uranium compounds, because photoemission results on plutonium and plutonium compounds to date are available only in angle-integrated mode, which prevents detailed E-vs-k investigations. We believe that photoemission investigations of the localization and hybridization of the $5f$ electrons in UAsSe might contribute to comprehension of the nature of the $5f$ electrons in the actinides.

In the following we briefly describe the experimental method in Sec. II and present experimental results in Sec. III.

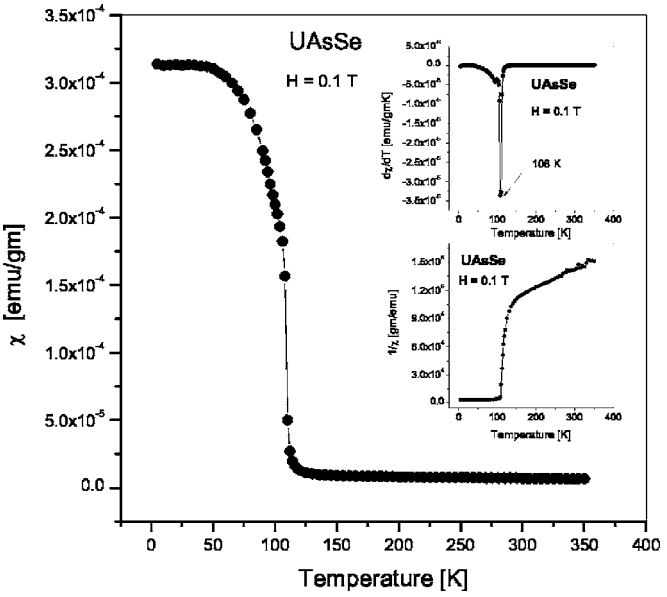

FIG. 2. Magnetic susceptibility of the UAsSe sample under investigation. The Curie temperature was determined as 108 K. Measurements of magnetization as a function of field at $T=5$ K (not shown here) revealed that magnetization saturates at a value smaller than but close to $1.5\mu_B$.

A comparison with *ab initio*—calculated energy bands is given in Sec. IV and discussed in Sec. V. Our conclusions are formulated in Sec. VI.

II. METHODS: EXPERIMENT

UAsSe single crystals were grown by the chemical vapor transport method using Br_2 as transporting agent. The photoemission results presented in the next paragraph were taken on the UAsSe sample with a Curie temperature of 108 K, as was determined from magnetic susceptibility measurements (Fig. 2). This corresponds to a sample with arsenic to selenium atomic ratio of about 0.95 (Ref. 14) and may indicate some disorder in the anionic sublattice.[16] In stoichiometric UAsSe, As and Se atoms are located on the different lattice sites and a random distribution of As and Se atoms has been excluded by a neutron scattering experiment.[39] For crystals with variations of the arsenic to selenide ratio some disorder in the anionic sublattice occurs as was indicated by x-ray and neutron diffraction experiments.[40]

Angle-resolved photoemission studies were performed at the Synchrotron Radiation Center of the University of Wisconsin in Stoughton. The tetragonal, layered type of UAsSe structure allows cleavage with very little surface disruption. Samples were cleaved and measured at 12 K under ultrahigh-vacuum conditions ($p \cong 10^{-11}$ Torr). The [001] surfaces were oriented by use of a Laue x-ray camera. The high quality of the samples was confirmed by the Laue patterns and by a clear sharp peak near the Fermi level (E_F).

The data were collected using the plane grating monochromator (PGM) beamline. ARPES data of UAsSe single crystals were taken at photon energies between 20 eV and 110 eV by an angle-resolved kinetic energy analyzer with

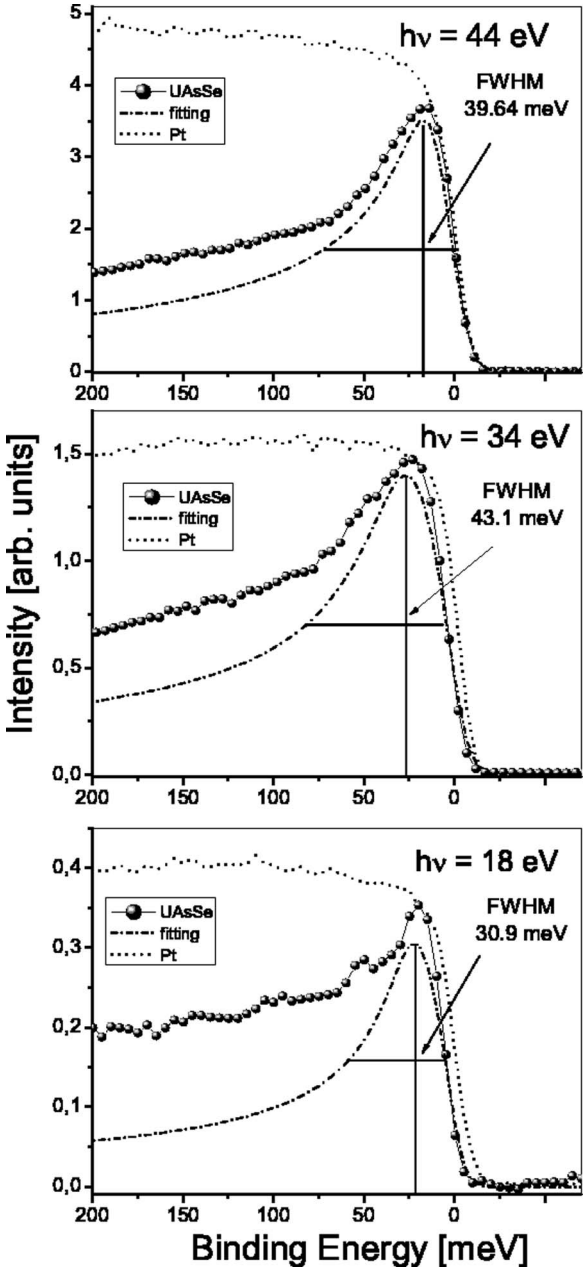

FIG. 3. The Fermi edge of platinum compared with near-E_F features of UAsSe. The peak of UAsSe is located very close to the Fermi edge. The dash-dotted line shows the fitting of the PES data of UAsSe.

±1° acceptance angle. The momentum resolution at $h\nu=30$ eV was about 0.09 Å^{-1}, which is about 12% of the Brillouin zone in the Γ to Z direction and about 6% in the Γ to X direction. The overall energy resolution varied between 14 meV for $h\nu=21.2$ eV and 22 meV for $h\nu=44$ eV. The position of the Fermi edge was established by Pt reference measurements to within 1 meV. Also, the resolution was determined from a Pt Fermi edge and the intensity at each binding energy point was normalized to the mesh current to account for synchrotron beam decay.

In Fig. 3 we show the Fermi edge of platinum compared with the near-E_F feature of UAsSe as obtained from our nor-

mal emission study. The dash-dotted line shows the fitting of the PES data shown as open circles. The instrumental resolution was determined from a numerical fitting of the Pt Fermi edge, and it was 13 meV for $h\nu$=18 eV, 18 meV for $h\nu$=34 eV, and 22 meV for $h\nu$=44 eV. It was always substantially below the Lorentzian full width at half maximum (FWHM) of the near-E_F feature of UAsSe, which at the lowest photon energy is about 28 meV. The UAsSe peak is extremely close to the Fermi edge and shows some small binding energy variations with photon energy. The shape of this peak varies strongly with $h\nu$, but for any photon energy we clearly observe an asymmetric, Doniach-Sunjic (DS) line shape. The DS line shape is typically observed in metals as a result of a long-life electron-hole response.[41,42] The numerical fitting of the UAsSe data shows that the DS asymmetry parameter is about 0.3. This value of the DS line shape is very close to that obtained for rare-earth compounds.[43] The dispersion of this peak as observed in normal emission and angular dependence spectra varies between 30 and 50 meV, which is significantly above both the instrumental resolution and Lorentzian FWHM as well. We also observe in Fig. 3 that the FWHM of the near-E_F peak does not follow a Fermi-liquid E^2 dependence of the linewidth. This seems to place the electronic structure of UAsSe outside of the Fermi-liquid regime.[44] A similar observation was made for USb_2 crystal.[45] However, it should be stressed that the near-E_F peak in UAsSe is significantly broader than the corresponding feature in USb_2, so the indication towards non-Fermi-liquid behavior should be taken with some care. There can be a few reasons for this. This peak might consist of two degenerated states as was observed for some directions in USb_2. Another explanation might be that its physical behavior is masked or it can be a result of processes extrinsic to a photoemission process.

III. EXPERIMENTAL RESULTS

We have measured ARPES spectra along selected high-symmetry directions in the Brillouin zone, covering the binding energy region of about 6 eV from the Fermi edge. Based on these results we were able to determine the effective inner potential of the UAsSe sample under investigation as 14.5 eV. For states at the Fermi level the Γ point of the Brillouin zone is accessible at photon energies of 25 eV and 44 eV, whereas the Z point is reached for photon energies of 17 eV or 34 eV in normal emission [see Fig. 1(b)]. In Figs. 4–7 we present the results of a photoemission investigation along Γ to Z, Γ to X, and Z to R [see Fig. 1(b)] directions of the Brillouin zone.

A. Normal emission: Γ to Z direction

In Fig. 4 we present a set of normal emission energy distribution curves of UAsSe taken at 12 K within 950 meV [Fig. 4(a)] and 150 meV [Fig. 4(b)] of the Fermi edge. The data were taken for photon energies between 18 eV and 46 eV. For UAsSe with c=8.402 Å and the inner potential of 14.5 eV this range of photon energies covers more than one Brillouin zone (BZ) along the Γ to Z direction. For $h\nu$

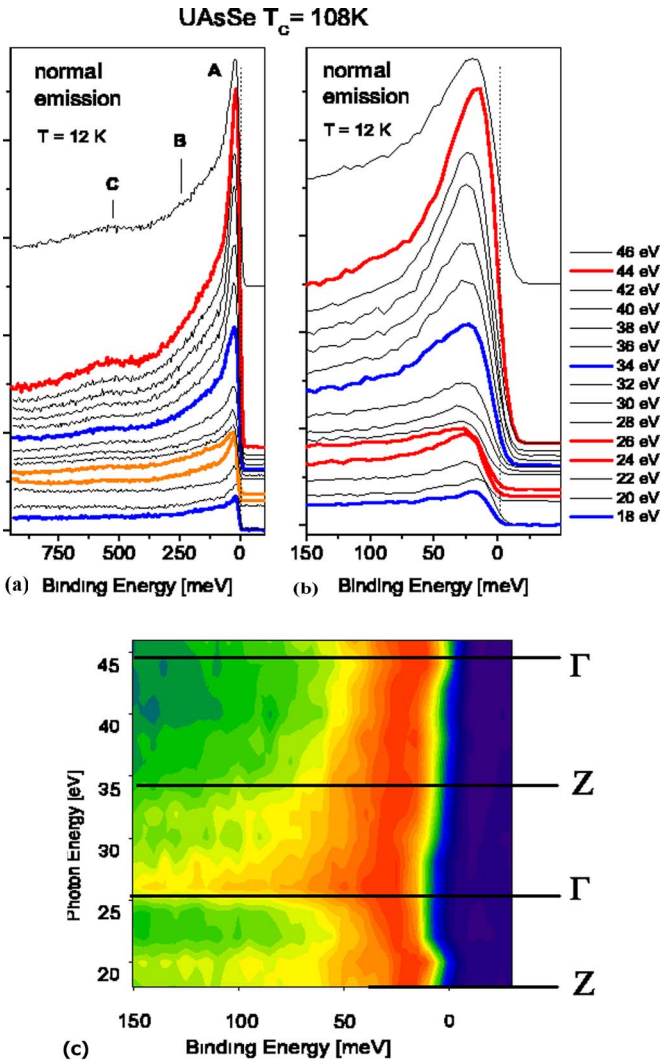

FIG. 4. (Color online) Normal-emission ARPES of UAsSe (Γ-Z direction in the Brillouin zone) taken at 12 K within 950 meV (a) and 150 meV (b) of the Fermi edge. Binding energy in (c) is the same as in (b), but the intensity is normalized to the maximum. Spectra marked in red show the spectra nearest to the Γ point of the Brillouin zone whereas spectra marked in blue show the Z point of the Brillouin zone.

=18 eV we are around the Z point. The Γ point is reached for $h\nu$=25 eV; at a photon energy of 34 eV, we are again at the Z point and for $h\nu$=44 eV, again at the Γ point. The EDC's which are closest to the Γ point are plotted in red whereas EDC's closest to the Z point are plotted in blue. In Fig. 4(a) we see two distinct peaks in the ARPES spectra. One of them (A) is located very close to the Fermi level, whereas the second one (C) about 550 meV below. The line shape of peak A evolves with photon energy, but in any case we observe the asymmetry of the peak and an additional contribution (structure B) at about 160 meV below E_F. The positions of B and C look the same for all investigated photon energies, but peak A disperses over a small binding energy range. The dispersion can be observed in Fig. 4(b) with an expanded binding energy scale. The dispersion, as seen from the numerical fitting, is about 25–30 meV. The value of the

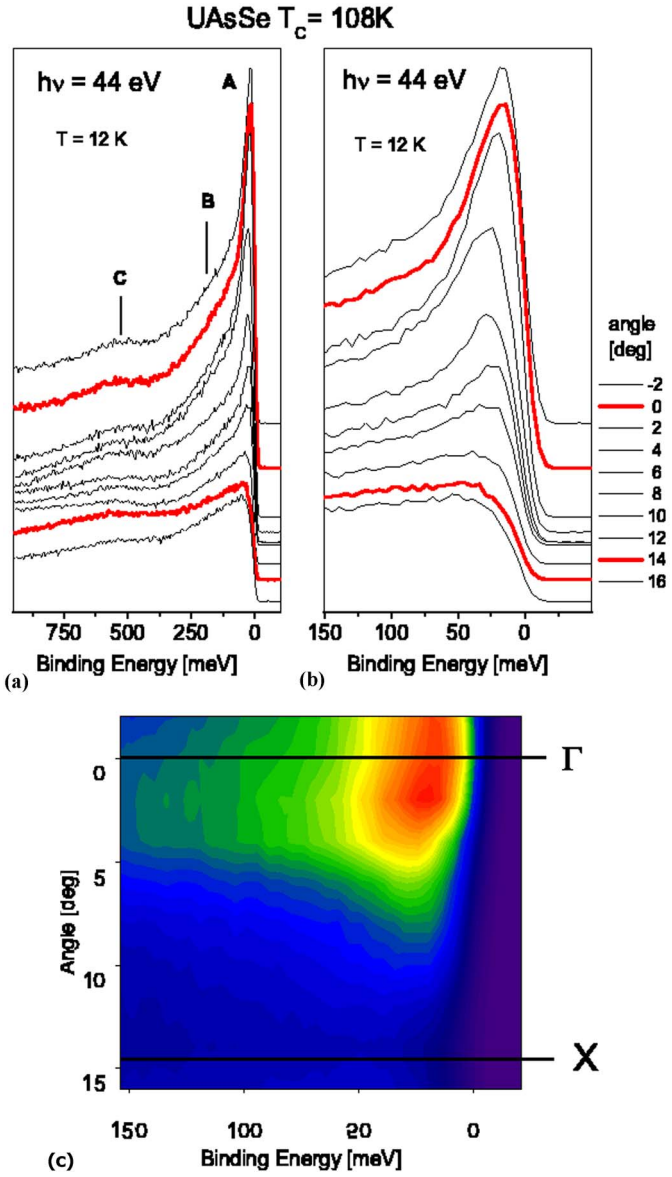

FIG. 5. (Color online) High-resolution ARPES spectra of UAsSe taken at a photon energy of 44 eV (Γ-*X* direction in the Brillouin zone) within 950 meV (a) and 150 meV (b) of the Fermi edge. Binding energy in (c) is the same as in (b), but the intensity is normalized to the maximum.

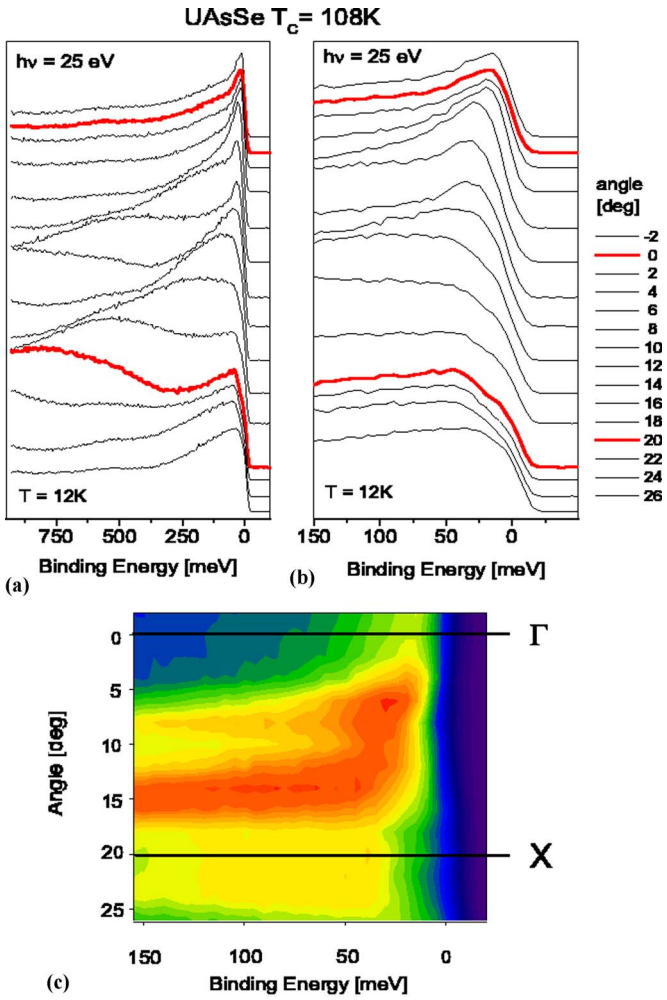

FIG. 6. (Color online) High-resolution ARPES spectra of UAsSe taken at a photon energy of 25 eV (Γ-*X* direction in the Brillouin zone) within 950 meV (a) and 150 meV (b) of the Fermi edge. Binding energy in (c) is the same as in (b).

dispersion is larger than the experimental resolution and much larger than our observable minimum energy shift. Peak *A*, along the Γ to *Z* direction, is situated between 5 meV (Γ point) and 30 meV below the Fermi level. The FWHM is about 25–28 meV for lower photon energies (18–28 eV) and about 35–40 meV for higher photon energies (30–46 eV). The Doniach-Sunjic asymmetry parameter was found to be about 0.3. This value is quite large, but not unprecedented in *f*-electron compounds.[43] In the fitting procedure we do not take into account the spin-orbit splitting. It might result in a slightly higher value of the obtained asymmetry parameter.

It should be noticed that the intensity of the peak at the Fermi level substantially increases with photon energy, which is not observed for the *B* and *C* structures. Based on a photoemission cross-section argument,[46] we assert that peak *A* is primarily of 5*f* character.

The dispersion observed in the normal-emission spectra provides evidence that the strong peak at the Fermi level is not a surface state, but rather a part of the bulk electronic structure. This finding also suggests that UAsSe, similar to other uranium-layer compounds such as USb_2, does not have a purely 2D electronic structure, but needs to be treated as a quasi-2D material.

B. Angular dependence: Γ to *X* direction

For uranium arsenoselenide the Γ point of the BZ is reached for $h\nu$=25 eV and 44 eV in normal-emission spectra. With photon energy of 25 eV we reach the vicinity of the *X* point for Θ=20°, whereas with $h\nu$=44 eV we are close to the *X* point for Θ=14°. In angular dependence studies presented in Secs. III B and III C we do not follow directly high-symmetry directions. Because we changed only the angle instead of changing the angle and photon energy si-

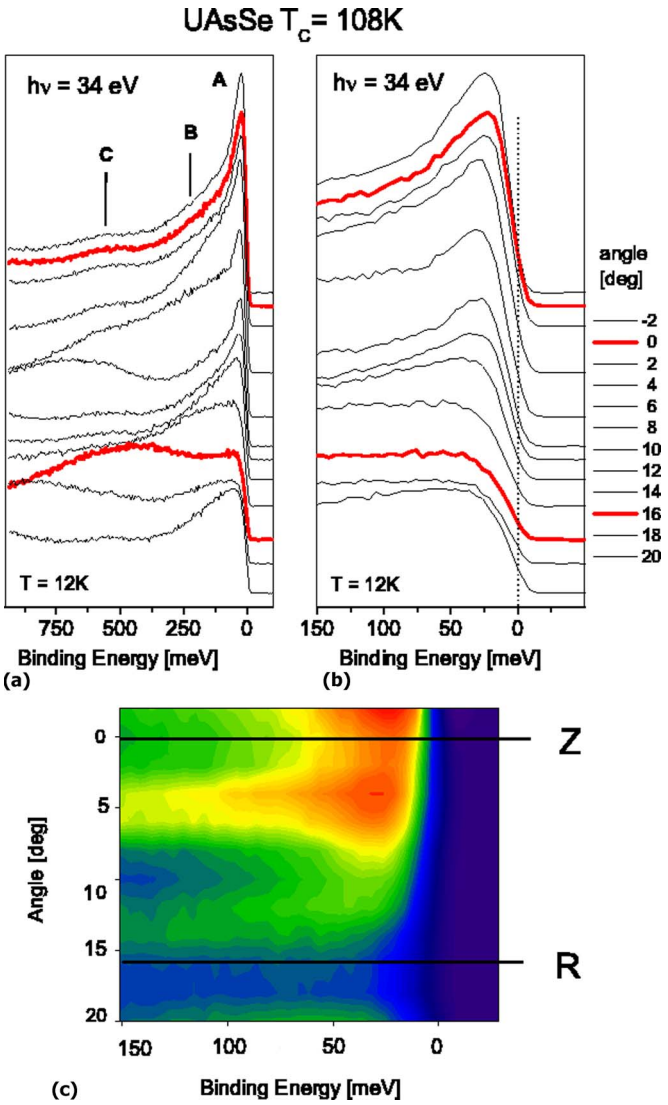

FIG. 7. (Color online) High-resolution ARPES spectra of UAsSe taken at a photon energy of 34 eV (*Z*-*R* direction in the Brillouin zone) within 950 meV (a) and 150 meV (b) of the Fermi edge. Binding energy in (c) is the same as in (b).

multaneously, we are about 24% off $k_\perp$ for $h\nu$=25 eV and Θ=20° and about 16% off $k_\perp$ for $h\nu$=44 eV and Θ=14°. However, we do not expect a big difference in the states sampled. UAsSe is a layered compound with a large c to a,b ratio, and normal-emission photoemission spectroscopy (PES) studies presented in the previous subsection showed that UAsSe is a quasi-2D material. Therefore we assume that the electronic states are only weakly dependent on $k_\perp$.

We investigated the Γ to X direction of the BZ taking ARPES spectra for the photon energy of both 44 eV and 25 eV. Photoionization cross sections for f and d electrons vary significantly in this photon energy range. For $h\nu$ =44 eV the cross section for 5f emission is about 10 times higher than that for 6d, so we believe that ARPES spectra measured with this photon energy show mainly the 5f electrons distribution. For $h\nu$=25 eV the cross section for the 6d-electron shell is about 50% higher than for the 5f shell, so we expect that ARPES spectra show mainly the 6d-electron energy dependence.

1. Angular dependence for $h\nu$=44 eV

In Fig. 5 we show ARPES spectra taken with photon energy of 44 eV. EDC's at the zone boundaries are marked in red. Within 950 meV from the Fermi edge [Fig. 5(a)] we observe peaks A (at the Fermi edge) and C (about 550 meV below E_F). We can also notice the contribution of the third structure (B), which is located 160 meV below the Fermi edge. The contribution of structure B is most pronounced for Θ=4°.

The intensity of the peak A drops very quickly for higher angles. At a photon energy of 44 eV the photoelectron cross section of the 5f states is much higher than of the 6d or every other electronic state in UAsSe. Therefore we assign the very high photoemission intensity at Θ=0° to the presence of the 5f electronic states.

ARPES spectra taken for $h\nu$=44 eV show that the 5f states are located mainly at (or near) the Γ point of the Brillouin zone. In Fig. 5(b) we see the ARPES spectra within 150 meV of the Fermi edge. The dispersion, as seen from numerical fitting, is about 40 meV. The band is about 5–10 meV below E_F at the Γ point and about 40–45 meV below E_F at the X point. The FWHM is 35–40 meV, and the Doniach-Sunjic asymmetry parameter was again found to be about 0.3.

2. Angular dependence for $h\nu$=25 eV

The EDC spectra taken for a photon energy of 25 eV [Fig. 6(a)] and Θ=0°–26° have a strong peak at the Fermi level, a weak structure about 550 meV below, and a third one situated at 160 meV, similarly as was for normal emission at $h\nu$=44 eV. The intensity of peak A is, however, much smaller. This indicates the 5f origin of structure A. Starting from Θ=8° at least two very dispersive structures appear in every EDC. One of them is observed at 300 meV for Θ =8°, at 550 meV for Θ=10°, and at about 625 meV for Θ =12°. The second one appears for higher angles: at 800 meV for Θ=20° (X point), 625 meV for Θ=18°, and about 275 meV for Θ=16°. These dispersive bands are not observed at the spectra taken for photon energy of 44 eV. Based on a photoemission cross section argument we propose for both these bands a dominant d character.

The peak nearest to the Fermi edge shows a dispersion of about 40 meV. At the Γ point it is 20 meV below E_F. For higher angles, when we approach the X point, it disperses towards higher binding energy and close to the X point it is 60 meV below the Fermi level. Unfortunately, in some cases (Θ=14–160°) the exact position of peak A is difficult to determine, as it is influenced by a very dispersive feature of d character, which probably crosses the Fermi level.

In Figs. 6(a) and 6(b) we do not see any substantial changes in the EDC's intensity. Peak A at the Fermi level and very dispersive structures several hundred meV below are of similar intensity, and we do not observe any dramatic change with the angle. Therefore we propose that both bands are of a dominating conduction electron character.

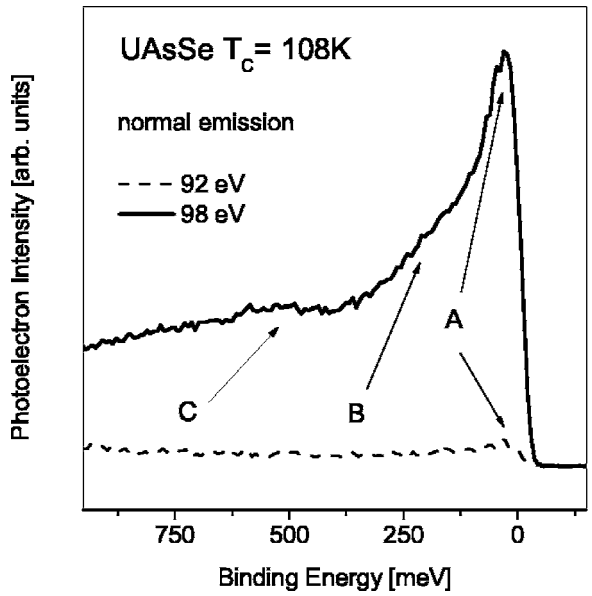

FIG. 8. Normal-emission spectra taken at Fano resonance ($h\nu$ =98 eV) and antiresonance ($h\nu$=92 eV) at 12 K.

C. Angular dependence: *Z* to *R* direction

In Figs. 7(a) and 7(b) we show the set of EDC's taken for $h\nu$=34 eV and Θ from −2° to 20°. At Θ=0° we are very close to the *Z* point and with increasing angle we approach the *R* points, which is almost reached for Θ=16°. The EDC spectra, which are the closest to the *Z* and *R* points, are marked in red. We evaluate that because we change only the angle with constant photon energy; for Θ=16°, we are about 20% off the *Z* point. Anyway, based on a quasi-2D character of UAsSe, we do not expect a significant difference in the states sampled as was explained in Sec. III B.

In Fig. 7(a) we observe very dispersive photoemission features, as in the case of the set of angular resolved spectra taken for $h\nu$=25 eV presented in Fig. 6(a). One band is the most pronounced at the *R* point (Θ=16°) and situated around 500 meV below the Fermi edge. For Θ=10°–140° it approaches the Fermi level and is within 100 meV of E_F. The second band appears for Θ=8° at 700 meV below the Fermi level.

The EDC spectra in the vicinity of the *Z* point look like the normal spectra observed for $h\nu$=44 eV (the Γ point). We can distinguish a sharp peak *A* at the Fermi edge, a much weaker peak *C* around 550 meV below, and a structure, labeled *B*, which is situated at about 160 meV below E_F. At the *Z* point peak *A* is around 20 meV below E_F and disperses by 40 meV towards lower binding energy as it approaches the *R* point.

The Lorentzian FWHM of peak *A*, as seen from the fitting, is about 30–40 meV with the Doniach-Sunjic parameter of about 0.33.

D. Resonant photoemission

In Fig. 8 we show normal-emission spectra measured at 12 K near the U $5d \rightarrow$ U $5f$ resonance. The photoemission spectrum taken at photon energy of 98 eV shows the resonant enhancement within 800 meV of the Fermi edge with maximum at 29 meV. The spectrum measured at a minimum of the resonance ($h\nu$=92 eV) is almost flat and shows only a very small structure at 30 meV below the Fermi edge. The shape of the EDC shows all the features observed in normal-emission EDC's taken for the photon energy range 18–46 eV. The EDC spectrum has a maximum near the Fermi level, a weak peak at 550 meV below, and additional structure at 160 meV. This means that all *A*, *B*, and *C* structures observed in normal-emission spectra have some admixture of $5f$ electrons. However, the strongest $5f$ contribution has peak *A* situated in the vicinity of the Fermi level. One should remember, however, that for photon energies between 92 eV and 98 eV we have a momentum resolution of about 0.16 Å^{-1} and the dimension of the Brillouin zone along the Γ to *Z* direction for UAsSe is 0.75 Å^{-1}. Therefore even for energies over 90 eV we still have some matrix element dependence. Photoemission spectra taken for 92 eV are in the vicinity of a Γ point, whereas spectra taken for 98 eV are in the vicinity of a *Z* point. Therefore the resonant photoemission results have only qualitative character.

Based on angular-resolved photoemission experiments, the emerging picture of the electronic band structure of uranium arsenoselenide is as follows. Within 50 meV below the Fermi level we observe a very slightly dispersive band located near the Γ point with Lorentzian FWHM of 35 meV. This narrow band is mainly of *f* character as was established based on resonant photoemission and cross-section dependences. It shows an important dispersion of 40 meV along the Γ to *X* direction and 30 meV dispersion along the Γ to *Z* direction of the Brillouin zone.

Apart from the narrow band we also observed at least two broader (FWHM about 70 meV) and highly dispersive bands below. They are of hybridized *f*-*d* character. These bands show conventional 1 eV dispersion along the Γ to *X* and *Z* to *R* directions, but no dispersion along the Γ to *Z* direction was observed.

IV. THEORETICAL EXPLANATION

A. Energy-band approach

The electronic structure of UAsSe has been computed within the framework of the local spin-density approximation (LSDA) to density functional theory. The calculations were performed using the relativistic augmented-spherical-wave (ASW) band structure method, adopting the von Barth–Hedin parametrization of the exchange-correlation potential (for details, see Ref. 21). The band structure calculations were carried out for both the ferromagnetic and nonmagnetic phases, assuming the experimental lattice parameters. The calculated total energy of ferromagnetically ordered UAsSe is lower than that of nonmagnetic UAsSe, in agreement with the observed ferromagnetic ground state. In terms of $5f$-electron occupancy, the paramagnetic calculation gives 3.10 *f* electrons and the ferromagnetic version results in 3.08 *f* electrons per uranium atom. In the latter approach there are 2.42 spin-up and 0.66 spin-down electrons. The calculated configuration is therefore close to $5f$.[3]

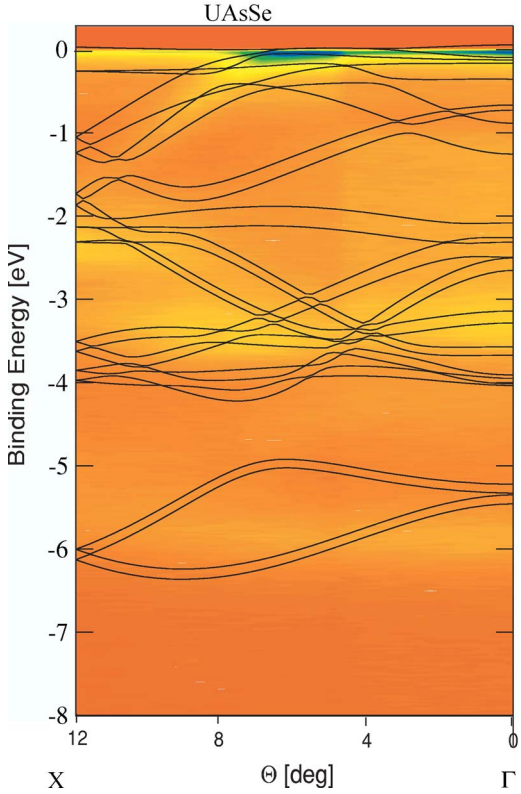

FIG. 9. (Color online) Comparison of the experimental ARPES energy-band spectrum (taken at $h\nu$=40 eV) and the computed LSDA energy bands, assuming full spin polarization. The experimental band positions are indicated by the colors, orange color depicting a low-energy-band response, blue color a high-energy-band intensity. Note the good overall agreement between the experimental and computed energy bands, including the 5*f* bands near the Fermi level.

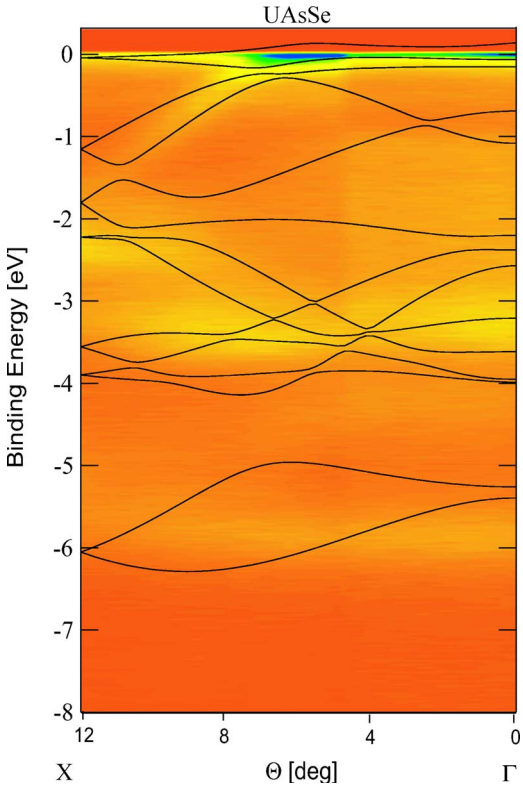

FIG. 10. (Color online) As Fig. 9, but showing the LSDA energy bands computed assuming no spin polarization. Some parts of the bands near the Fermi edge are better captured.

B. Comparison of experimental and calculated energy bands

To compare the experimental and computed energy bands we have measured ARPES spectra on a wide energy interval, down to binding energies of about 8 eV. This energy window will certainly comprise the dispersive energy bands, for which energy-band theory should be applicable. The nearly dispersionless *f* bands in the immediate vicinity of the Fermi level can be strongly modified through pertinent electron correlations, and it is a question how well they can be explained by LSDA energy bands. Our ARPES data presented in this subsection were collected on a UAsSe sample with a T_C of 113 K, using photon energies of 40 and 60 eV. For $h\nu$ =60 eV the photoionization cross sections favor mainly *f* emission and *d* emission is negligible. For $h\nu$=40 eV, *f* emission dominates, but *d* emission is noticeable and should be taken into account. Neither for $h\nu$=60 eV nor for $h\nu$ =40 eV are we at the high-symmetry points (*Z* or Γ), but because of the quasi-2D character of the electronic structure (confirmed by normal emission studies), we expect a similar electronic structure along the high-symmetry lines Γ to *X* and *Z* to *R*. The instrumental resolution for these measurements was about 30 meV. The energy bands mapped onto reciprocal space are shown in Figs. 9 and 10. The reciprocal-space part shown corresponds to a section of Brillouin zone along the Γ to *X* direction. The colors denote the intensity of the emissions: a blue color indicates strong intensities and a orange color low intensities. The 5*f* band is seen as the green-blue intensity near the Fermi level. Other dispersive bands which are displayed as yellow can be recognized as well. These bands are dispersed by several eV in reciprocal space. As mentioned before, the band approaching the Fermi edge from about 2 eV binding energy at θ=24° is of mixed *d*-*f* character. This band hybridizes with the 5*f*-related band in the region about θ=14°, which then crosses the Fermi level, but reappears at about θ=8° below E_F. This is a classic example of *d*-*f* hybridization.

The LSDA-calculated energy bands,[21] shown in Figs. 9 and 10, correctly describe most of the measured bands. The bands at binding energies below 2 eV are properly placed and so are the *f* band and the dispersive hybridized *d*-*f* band. It seems as if the experimental bands are somewhat narrower than the computed bands (see, e.g., the calculated and experimental bands at 3–4 eV binding energy). Also the *s*-derived bands at 5–6 eV binding energy appear to be somewhat deeper in the calculation than in experiment. The aspects of the *d*-*f* hybridization are well given by the LSDA energy-band theory, which becomes most evident when the *f* bands without exchange splitting are considered (Fig. 10): the *f* band closest to, but below, the Fermi level turns up to above E_F at θ=14°, precisely as seen experimentally. This is the region where the dispersive band of mixed *d*-*f* character hybridizes with the *f* bands. For angles of about 8° the *f*-like

band bends down towards the Fermi level, but remains just above E_F in the calculation. In the region where experimentally the high f-emission intensity is observed it comes closest to the Fermi level ($\theta \sim 6°$).

V. DISCUSSION

Our ARPES measurements reveal intriguing properties of the f-electron states in UAsSe. High-resolution measurements allow the observation of a narrow band of $5f$ character situated within 50 meV from the Fermi energy. This narrow $5f$ band exhibits some dispersion; therefore, it is distinct from an atomiclike, localized $5f$ level. Nonetheless, the observation of this $5f$ band indicates a tendency towards f localization in UAsSe. The observation of the d-f-hybridized bands with a conventional dispersion of a few eV demonstrates that broader bands containing typically delocalized f electrons do occur in the same material. Our observations beautifully reflect the dual nature of actinide f electrons, which was postulated many years ago (see, e.g., Refs. 1 and 2), with the distinction that we observe both a very narrow $5f$ band and a dispersive $5f$ band in *one* material. It should, however, be stressed that the situation of the localization of the $5f$ band in UAsSe is still far from that in δ-Pu (Ref. 35) or $PuCoGa_5$ (Ref. 36) where a part of the $5f$ electrons seem to localize and form multiplet close to the Fermi level.

The degree of $5f$ localization in UAsSe has been controversially discussed in the literature.[11,17–19,22] A good comparison of the measured[17] and *ab initio*–calculated[21] magneto-optical spectra of UAsSe provided evidence that the $5f$ electrons in UAsSe are at least partially delocalized. The agreement between the *ab initio*–calculated and experimental Kerr spectra is similar to the agreement normally obtained for itinerant transition-metal compounds.[47,48] Since magneto-optical Kerr spectra in the polar geometry sensitively probe the electronic structure in the planes perpendicular to the c axis, it was suggested that the $5f$ electrons in the uranium planes are rather delocalized.[21] This conjecture is consistent with our ARPES data; the measured energy-band dispersions match well to the ones calculated with the LSDA-delocalized approach. The dispersion of the f band near E_F could experimentally be smaller than in the LSDA calculation, but such a minor difference would not become visible in the magneto-optical spectrum which was convoluted with a Lorentzian of 0.4 eV width to simulate lifetime broadening.[21]

Magneto-optical spectroscopy (with incident light along the c axis) only probes the $5f$ electrons in the uranium planes. It was proposed[21] that a higher degree of localization could possibly exist for $5f$ electrons perpendicular to the uranium planes. A later polarized-neutron diffraction study could, however, not detect an anisotropy of the uranium-atom magnetic form factor.[20] Our high-resolution photoemission results do, conversely, indicate that the $5f$ electrons are indeed less hybridized in the c direction (Γ to Z direction) and more hybridized (delocalized) in the uranium planes (Γ to X and Z to R directions in the Brillouin zone).

A comparison of Figs. 9 and 10 indicates that the non-spin-polarized energy-band structure fits better to the experimental data. For this observation we do not have a complete explanation. Since different samples were used for the ARPES measurements, it could be that some As/Se disorder played a role. Spin polarization of the bands is beyond doubt: The magneto-optical signal depends on the spin polarization,[48] and since the measured[17,22] and calculated[21] magneto-optical Kerr effects have the same magnitude, the amount of spin polarization of the bands appears to correspond reasonably well.

VI. CONCLUSIONS

We have investigated the hard ferromagnet UAsSe by angle-resolved high-resolution photoemission. We have found a relatively sharp peak of $5f$ character in the vicinity of the Fermi level. The Lorentzian FWHM of this peak is about 35 meV. Thus, this electron state is localized in the vicinity of the Γ point and situated about 5 meV below the Fermi level. When we move from the Γ point to the Z point, the peak looses over 80% of its intensity and disperses by 30 meV towards higher binding energy. When we move from the Γ point towards the X point the dispersion is 40 meV and at the X point the peak intensity is about 75% of the intensity at the Γ point.

Apart from the $5f$ band well localized a few meV below the Γ point, we have also observed a highly dispersive band of hybridized d-f character. The dispersion is about 1 eV both along the Γ-X and Z-R directions. No dispersion along the Γ-Z direction was found. Thus, our ARPES data reveal the fascinating, dual nature of $5f$-electron states in UAsSe: The occurrence of both dispersive and almost dispersionless $5f$ states has been observed in one actinide material. The $5f$ band nevertheless shows some reciprocal-space dispersion; therefore, it cannot be described as a purely localized state. Instead, its description requires lattice periodicity to be accounted for. Energy-band theory on the basis of the LSDA provides a remarkably good explanation of both the hybridized (delocalized) and almost unhybridized (nearly localized) $5f$ bands. The agreement between the measured and calculated energy bands stipulates that the LSDA energy-band approach sufficiently well describes the dual nature of the $5f$ electrons in UAsSe.

Our photoemission results confirm, last, the conclusion based on the magneto-optical Kerr effect calculations[21] that the $5f$ electrons are less hybridized along the c axis (Γ to Z direction in the Brillouin zone) and hybridized (itinerant) in the uranium planes (Γ to X and Z to R directions in the Brillouin zone).

ACKNOWLEDGMENTS

This work was supported by the U.S. Department of Energy, Office of Science, Division of Materials Science and Engineering, under Contract No. W-7405-ENG-82. This work is based upon research conducted at the Synchrotron Radiation Center, University of Wisconsin-Madison, which is supported by the NSF under Award No. DMR-0084402. E.G. was supported by the LANL Seaborg Institute.

*Corresponding author. Electronic address: Elzbieta.Guziewicz@ifpan.edu.pl

[1] H. H. Hill, Nucl. Metall. **17**, 2 (1970).
[2] A. J. Freeman and D. D. Koelling, in *The Actinides: Electronic Structure and Related Properties*, edited by A. J. Freeman and J. B. Darby, Jr. (Academic Press, New York, 1974).
[3] V. Sechovský and L. Havela, in *Handbook of Magnetic Materials*, edited by K. H. J. Buschow (North-Holland, Amsterdam, 1998), Vol. 11, pp. 1–289.
[4] D. D. Koelling, B. D. Dunlap, and G. W. Crabtree, Phys. Rev. B **31**, 4966 (1985).
[5] P. Santini, R. Lemanski, and P. Erdös, Adv. Phys. **48**, 537 (1999).
[6] T. Gouder, F. Wastin, J. Rebizant, and L. Havela, Phys. Rev. Lett. **84**, 3378 (2000).
[7] T. Durakiewicz, C. D. Batista, J. D. Thompson, C. G. Olson, J. J. Joyce, J. E. Gubernatis, E. Guziewicz, M. T. Butterfield, A. J. Arko, J. Bonča, K. Mettenberger, and O. Vogt, Phys. Rev. Lett. **93**, 267205 (2004).
[8] C. D. Batista, J. Bonča, and J. E. Gubernatis, Phys. Rev. B **68**, 064403 (2003).
[9] C. D. Batista, J. Bonča, and J. E. Gubernatis, Phys. Rev. B **68**, 214430 (2003).
[10] D. J. Garcia, K. Hallberg, C. D. Batista, and M. Avignon, Phys. Rev. Lett. **85**, 3720 (2000).
[11] J. Brunner, M. Erbudak, and F. Hulliger, Solid State Commun. **38**, 841 (1981).
[12] Z. Henkie, A. Pietraszko, A. Wojakowski, L. Kępiński, and T. Cichorek, J. Alloys Compd. **317–318**, 52 (2001).
[13] T. Cichorek, Z. Henkie, P. Gegenwart, M. Lang, A. Wojakowski, M. Dischner, and F. Steglich, J. Magn. Magn. Mater. **226–230**, 189 (2001).
[14] Z. Henkie, R. Fabrowski, A. Wojakowski, and A. J. Zaleski, J. Magn. Magn. Mater. **140–144**, 1433 (1995).
[15] Z. Henkie, T. Cichorek, R. Fabrowski, A. Wojakowski, B. S. Kuzhel, Cz. Marucha, M. S. Szczepaniak, and J. Tadla, Physica B **281–282**, 226 (2000).
[16] T. Cichorek, Z. Henkie, A. Wojakowski, A. Pietraszko, P. Gegenwart, M. Lang, and F. Steglich, Solid State Commun. **121**, 647 (2002).
[17] W. Reim, J. Schoenes, and F. Hulliger, Physica **130B**, 64 (1985).
[18] A. Zygmunt and M. Duczmal, Phys. Status Solidi A **9**, 659 (1972).
[19] K. P. Bielov, A. S. Dmitrievskii, A. Zygmunt, R. Z. Levitin, and V. Trzebiatowski, Sov. Phys. JETP **37**, 297 (1973).
[20] P. Wiśniewski, A. Gukasov, Z. Henkie, and A. Wojakowski, J. Phys.: Condens. Matter **11**, 6311 (1999).
[21] P. M. Oppeneer, M. S. S. Brooks, V. N. Antonov, T. Kraft, and H. Eschrig, Phys. Rev. B **53**, R10437 (1996).
[22] W. Reim, J. Magn. Magn. Mater. **58**, 1 (1986).
[23] A. Wojakowski, Z. Henkie, and Z. Kletowski, Phys. Status Solidi A **14**, 517 (1972).
[24] Z. Henkie, R. Fabrowski, and A. Wojakowski, J. Alloys Compd. **219**, 248 (1995).
[25] Z. Henkie, A. Wojakowski, T. Cichorek, R. Wawryk, A. B. Maple, E. D. Bauer, and F. Steglich, Physica C **387**, 113 (2003).
[26] D. L. Cox and A. Zawadowski, Adv. Phys. **47**, 599 (1998).
[27] T. Cichorek, A. Sanchez, P. Gegenwart, F. Weickert, A. Wojakowski, Z. Henkie, G. Auffermann, S. Paschen, R. Kniep, and F. Steglich, Phys. Rev. Lett. **94**, 236603 (2005).
[28] A. J. Arko, J. J. Joyce, J. L. Sarrao, J. D. Thompson, L. A. Morales, Z. Fisk, A. Wojakowski, and T. Cichorek, J. Supercond. **12**, 175 (1999).
[29] A. J. Arko, J. J. Joyce, D. P. Moore, J. L. Sarrao, L. A. Morales, T. Durakiewicz, Z. Fisk, D. D. Koelling, and C. G. Olson, J. Electron Spectrosc. Relat. Phenom. **117–118**, 323 (2001).
[30] J. C. Lashley, A. Lawson, R. J. McQueeney, and G. H. Lander, Phys. Rev. B **72**, 054416 (2005).
[31] J. Bouchet, B. Siberchicot, F. Jollet, and A. Pasturel, J. Phys.: Condens. Matter **12**, 1723 (2000).
[32] S. Y. Savrasov, G. Kotliar, and E. Abrahams, Nature (London) **410**, 793 (2001).
[33] P. Soderlind, A. L. Landa, and B. Sadigh, Phys. Rev. B **66**, 205109 (2002).
[34] A. J. Arko, J. J. Joyce, L. Morales, J. Wills, J. Lashley, F. Wastin, and J. Rebizant, Phys. Rev. B **62**, 1773 (2000).
[35] J. M. Wills, O. Eriksson, A. Delin, P. H. Andersson, J. Joyce, T. Durakiewicz, M. Butterfield, A. Arko, D. Moore, and L. Morales, J. Electron Spectrosc. Relat. Phenom. **135**, 163 (2004).
[36] J. J. Joyce, J. M. Wills, T. Durakiewicz, M. T. Butterfield, E. Guziewicz, J. L. Sarrao, L. A. Morales, A. J. Arko, and O. Eriksson, Phys. Rev. Lett. **91**, 176401 (2003).
[37] E. Runge, P. Fulde, D. V. Efremov, N. Hasselmann, and G. Zwicknagl, Phys. Rev. B **69**, 155110 (2004).
[38] D. V. Efremov, N. Hasselmann, E. Runge, P. Fulde, and G. Zwicknagl, Phys. Rev. B **69**, 115114 (2004).
[39] J. Leciejewicz and A. Zygmunt, Phys. Status Solidi A **13**, 657 (1972).
[40] Z. Henkie, T. Cichorek, A. Pietraszko, R. Fabrowski, A. Wojakowski, B. S. Kuzhel, L. Kępiński, L. Krajczyk, A. Gukasov, and P. Wiśniewski, J. Phys. Chem. Solids **59**, 385 (1998).
[41] G. K. Wertheim and P. H. Citrin, in *Photoemission in Solids I*, edited by M. Cardona and L. Ley (Springer-Verlag, Berlin, 1978), Chap. 5, pp. 197–225.
[42] J. J. Joyce, M. del Giudice, and J. H. Weaver, J. Electron Spectrosc. Relat. Phenom. **49**, 31 (1989).
[43] J. J. Joyce, A. B. Andrews, A. J. Arko, R. J. Bartlett, R. I. R. Blyth, C. G. Olson, P. J. Benning, P. C. Canfield, and D. M. Poirier, Phys. Rev. B **54**, 17515 (1996).
[44] G. R. Stewart, Rev. Mod. Phys. **73**, 797 (2001).
[45] E. Guziewicz, T. Durakiewicz, M. T. Butterfield, C. G. Olson, J. J. Joyce, A. J. Arko, J. L. Sarrao, D. P. Moore, and L. Morales, Phys. Rev. B **69**, 045102 (2004).
[46] J. J. Yeh and I. Lindau, *Atomic Data and Nuclear Tables* (Academic Press, New York, 1985), Vol. 32, pp. 53, 54, and 112.
[47] P. M. Oppeneer, T. Maurer, J. Sticht, and J. Kubler, Phys. Rev. B **45**, 10924 (1992).
[48] P. M. Oppeneer, in *Handbook of Magnetic Materials*, edited by K. H. J. Buschow (Elsevier, Amsterdam, 2001), Vol. 13, p. 229.